Introduction into fracture and damage mechanics for rock mechanical applications

Authors: Prof. Dr. habil. Heinz Konietzky, Dr. rer. nat. Martin Herbst (TU Bergakademie Freiberg, Geotechnical Institute)

Introduction into fracture and damage mechanics for rock mechanical applications

Only for private and internal use!   Updated: 4 January 2021

1   Introduction at the atomic level

Two neighboring atoms are in a position of rest, if they are at the energy-related lowest level, which means, that attractive and repulsive forces are in equilibrium.

The atomic binding energy E can be described as follows (see Fig. 1.1):
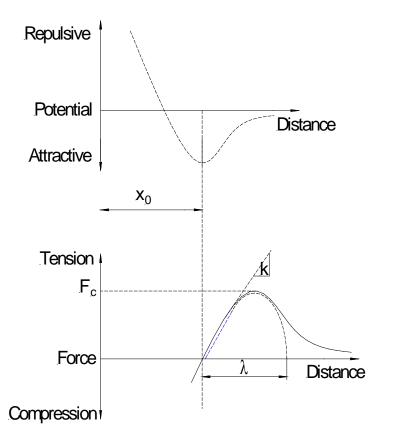
$$E = \int_{x_0}^{\infty} F \cdot dx \qquad (1.1)$$

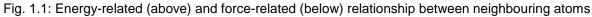In a simplified manner, the force history can be described by a sinus function according x to:

$$F = F_c \cdot \sin\left(\frac{\pi \cdot x}{\lambda}\right) \qquad (1.2)$$

In good approximation Eq. 1.2 can be linearized:

$$F \approx F_c \cdot \frac{x}{\lambda} \qquad (1.3)$$

Under the assumption of a linear force displacement relation the stiffness K can be introduced:

Fig. 1.1: Energy-related (above) and force-related (below) relationship between neighbouring atoms

Introduction into fracture and damage mechanics for rock mechanical applications

Only for private and internal use!   Updated: 4 January 2021

$$F \approx F_c \cdot \frac{x}{\lambda} = K \cdot x \qquad (1.4)$$

Re-arrangement of Eq. 1.4 leads to the definition of stiffness K:

$$K \approx \frac{F_c}{\lambda} \qquad [K] = \text{N/m} \qquad (1.5)$$

If one relates force and stiffness to the basic length and basic area (multiplication with x_0 and division by basic area) Eq. 1.5 leads to a Hook's relation for the tensile strength σ_c:

$$E \approx \frac{\sigma_c \cdot x_0}{\lambda} \qquad (1.6)$$

Under the assumption that $x_0 \approx \lambda$ Eq. 1.6 yields:

$$\sigma_c \approx E \qquad (1.7)$$

According to Eq. 1.7, the tensile strength of rocks (and solids in general) should have the same order of magnitude as the corresponding Young's moduls. This is in contrast to the practical experience: Young's moduls of rocks are in the order of several 10 GPa, whereas the tensile strength has only values of a few MPa. This discrepancy (factor of about 1000) can be explained by the existence of defects (pores, micro cracks, flaws etc.) at the micro and meso scale.

The relations shown in Fig. 1.1 can also be interpreted in terms of energy by the so-called specific surface energy γ, which is equal to the one half of the fracture energy, because two new surfaces are created during the fracturing process. If we relate the force F to the corresponding stress σ an expression for γ can be obtained:

$$2\gamma = \int_0^\lambda \sigma(x)\,dx = \int_0^\lambda \sigma_c \cdot \sin\left(\frac{\pi \cdot x}{\lambda}\right)\,dx = \sigma_c \frac{2\lambda}{\pi} \qquad [\gamma] = \frac{\text{Nm}}{\text{m}^2} \qquad (1.8)$$

If Equation 1.8 is inserted into Equation 1.7 one obtains:

$$\gamma = \frac{E \cdot \lambda}{\pi} \qquad (1.9)$$

Further rearrangement of Eq. 1.8 lead to the following expression:

$$\sigma_c = \frac{\gamma \cdot \pi}{\lambda} \qquad (1.10)$$

To handle the phenomenon of reduced strength and to consider the effect of defects the theoretical concepts of fracture and damage mechanics were developed.

Introduction into fracture and damage mechanics for rock mechanical applications

Only for private and internal use!   Updated: 4 January 2021

2   Basic terms of fracture mechanics

The classical fracture mechanical concept is mainly based on stress concentrations at the crack tips and can be deduced from the "Inglis"-solution under the assumption, that one half axis of the ellipsoidal opening (e.g. a micropore) approaches zero.

The extremum of the tangential stress at the boundary at $\beta = 0°$ is given by the following formulae (Fig. 2.1):

$$\sigma_t = -\frac{(1-\lambda)f + 2}{f}\,p \qquad \text{with} \quad f = \frac{b}{a} \tag{2.1}$$

For $b \to 0$ arises a flat ellipse, which degenerates towards a horizontal fracture:

$$b \to 0 \quad \Rightarrow \quad f \to 0 \quad \Rightarrow \quad \sigma_t(\beta = 0) \to \infty \tag{2.2}$$

According to Eq. 2.1 and 2.2, the tangential stress immediately at the crack tip is virtually infinite. The exact representation of the stress field around the crack tip is given by the „Griffith" crack model according to Fig. 2.2.
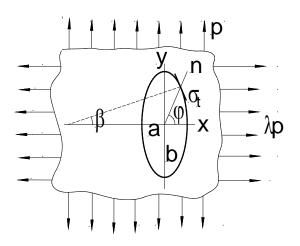

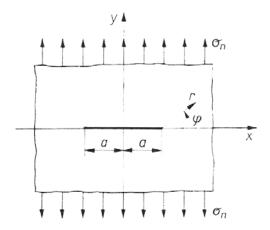Fig. 2.1: Modell of an elliptical pore under anisotropic tension
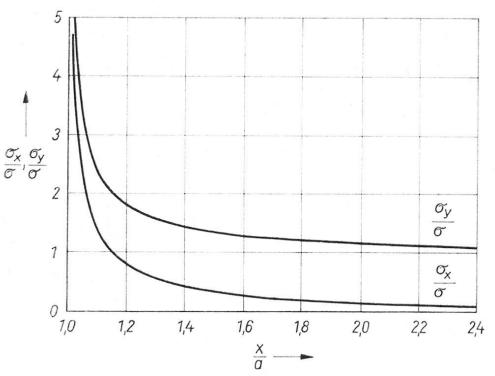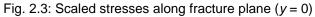

Fig. 2.2: Griffith model

The „Griffith" crack model considers a plane crack of length 2a inside an infinite plate. The stress field can be obtained by the so-called complex stress functions of "Kolosov". The stress field along the horizontal line y=0 ahead of the crack tip is given by the following expressions, which are graphically shown in Fig. 2.3:

$$\sigma_x\left(\frac{x}{a} \geq 1; y = 0\right) = \sigma\left[\frac{\dfrac{x}{a}}{\sqrt{\left(\dfrac{x}{a}\right)^2 - 1}} - 1\right] \tag{2.3}$$

$$\sigma_y\left(\frac{x}{a} \geq 1; y = 0\right) = \sigma\frac{\dfrac{x}{a}}{\sqrt{\left(\dfrac{x}{a}\right)^2 - 1}} \tag{2.4}$$

Fig. 2.3: Scaled stresses along fracture plane ($y = 0$)

Introduction into fracture and damage mechanics for rock mechanical applications

Only for private and internal use! Updated: 4 January 2021

For the area very close to the crack tip ($\frac{r}{a} \ll 1$) the following approximation is valid:

In Cartesian coordinates:

$$\begin{pmatrix} \sigma_x \\ \sigma_y \\ \tau_{xy} \end{pmatrix} = \sigma \sqrt{\frac{a}{2r}} \begin{pmatrix} \cos\frac{\varphi}{2}\left[1 - \sin\frac{\varphi}{2}\sin\frac{3\varphi}{2}\right] \\ \cos\frac{\varphi}{2}\left[1 + \sin\frac{\varphi}{2}\sin\frac{3\varphi}{2}\right] \\ \sin\frac{\varphi}{2}\cos\frac{\varphi}{2}\cos\frac{3\varphi}{2} \end{pmatrix} \tag{2.5}$$

In cylindrical coordinates:

$$\begin{pmatrix} \sigma_r \\ \sigma_\varphi \\ \tau_{r\varphi} \end{pmatrix} = \frac{\sigma}{4}\sqrt{\frac{a}{2r}} \begin{pmatrix} 5\cos\frac{\varphi}{2} - \cos\frac{3\varphi}{2} \\ 3\cos\frac{\varphi}{2} + \cos\frac{3\varphi}{2} \\ \sin\frac{\varphi}{2} + \sin\frac{3\varphi}{2} \end{pmatrix} \tag{2.6}$$

The stress field at the crack tip is illustrated in Fig. 2.4. From Eq. 2.5 and 2.6, respectively, it becomes obvious, that the term $\sigma \cdot \sqrt{a}$ is a characteristicc value to describe the intensity of the stress state at the crack tip, i. e.

$$\sigma_{crack\_tip} \sim \sigma_{far\_field} \tag{2.7}$$
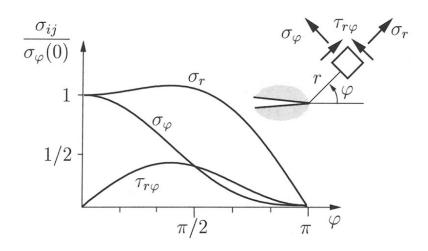
$$\sigma_{crack\_tip} \sim \sqrt{a} \tag{2.8}$$

Fig. 2.4: Stress field at the crack tip in Mode I (pure tensile crack)

Introduction into fracture and damage mechanics for rock mechanical applications

Only for private and internal use!   Updated: 4 January 2021

The important fracture mechanical parameter K (stress intensity factor) can be deduced also from Eq. 2.5 and 2.6:

$$K_I = \sigma \cdot \sqrt{\pi \cdot a} \qquad [K_I] = \text{Pa} \cdot \sqrt{\text{m}} \tag{2.9}$$

K_I characterizes the stress concentration at the crack tip for Mode I (tensile crack). In general the following is valid:

$$K = \sigma \cdot \sqrt{\pi \cdot a} \cdot Y \tag{2.10}$$

Y is a dimensionless factor, which considers geometry and mode of loading. Exemplary, Fig. 2.5 shows a specific crack constellation and Eq. 2.11 shows the expression for the corresponding stress intensity factor. In case of infinite length of sample W, Eq. 2.12 can be used. Several text books provide solutions for Y for quite different crack and loading configurations (e.g. Anderson 1995, Gross & Seelig 2001, Gdoutos 2005).

$$K_I \approx 1{,}122 - 0{.}231\frac{a_m}{W} + 10{.}55\left(\frac{a_m}{W}\right)^2 - 21{.}71\left(\frac{a_m}{W}\right)^3 + 30{.}382\left(\frac{a_m}{W}\right)^4 \tag{2.11}$$

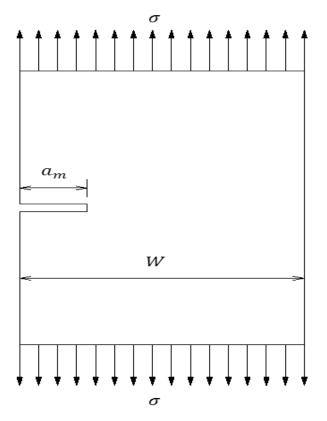$$K_I \approx 1{,}122 \cdot \sigma \cdot \sqrt{\pi \cdot a} \qquad \text{for} \qquad w \to \infty \tag{2.12}$$

Fig. 2.5: Plane under unixial σ tension with initial crack of length a at the left hand boundary

Introduction into fracture and damage mechanics for rock mechanical applications

Only for private and internal use!   Updated: 4 January 2021

Eq. 2.5 can be re-written using the stress intensity factor:

$$\begin{pmatrix} \sigma_x \\ \sigma_y \\ \tau_{xy} \end{pmatrix} = \frac{K_I}{\sqrt{2\pi r}} \begin{pmatrix} \cos\frac{\varphi}{2}\left[1 - \sin\frac{\varphi}{2}\sin\frac{3\varphi}{2}\right] \\ \cos\frac{\varphi}{2}\left[1 + \sin\frac{\varphi}{2}\sin\frac{3\varphi}{2}\right] \\ \sin\frac{\varphi}{2}\cos\frac{\varphi}{2}\cos\frac{3\varphi}{2} \end{pmatrix} \tag{2.13}$$

Beside tensile fracture (Mode I) two other basic fracture types can be distinguished (Fig. 2.6):

– Mode II: shear fracture (in-plane shear)

– Mode III: torsion fracture (out-of-plane shear)

Due to often 3-dimensional loading and inclined orientation of cracks in respect to loading directions mixed-mode fracturing takes place. The stress field at the crack tip for such constellations can be given by the following formulae:

$$\sigma_{ij} = \frac{1}{\sqrt{2\pi r}} \left[K_I F_{ij}^I(\varphi) + K_{II} F_{ij}^{II}(\varphi) + K_{III} F_{ij}^{III}(\varphi) \right], \tag{2.14}$$

where $F_{ij}(\varphi)$ contains angular functions valid for the different fracture modes.

Alternative to the stress field description the so-called energy release rate G can be used. G gives the energy loss per crack propagation ($Nm/m^2 = N/m$). For linear elastic material in 2D the following expressions are valid:
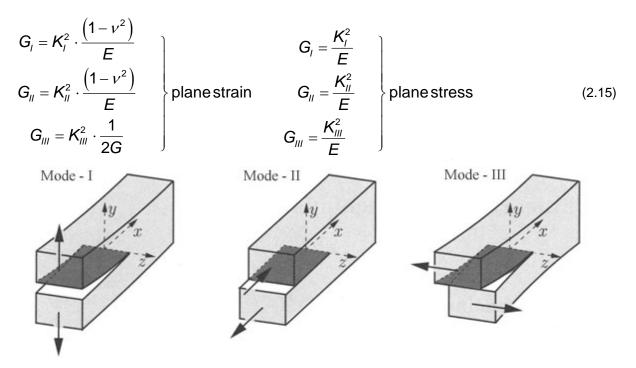
$$\left.\begin{aligned} G_I &= K_I^2 \cdot \frac{(1-v^2)}{E} \\ G_{II} &= K_{II}^2 \cdot \frac{(1-v^2)}{E} \\ G_{III} &= K_{III}^2 \cdot \frac{1}{2G} \end{aligned}\right\} \text{plane strain} \qquad \left.\begin{aligned} G_I &= \frac{K_I^2}{E} \\ G_{II} &= \frac{K_{II}^2}{E} \\ G_{III} &= \frac{K_{III}^2}{E} \end{aligned}\right\} \text{plane stress} \tag{2.15}$$

Fig. 2.6: Fracture mode I (opening mode) , II (sliding mode) and III (tearing mode)

Introduction into fracture and damage mechanics for rock mechanical applications

Only for private and internal use!   Updated: 4 January 2021

The above outlined theory is restricted to linear elastic material behaviour and called LEFM (Linear Elastic Fracture Mechanics). A more general parameter is the so-called J-Integral, which is also valid for any kind of non-linear behavior. For linear elastic behavior (LEFM) and plane strain condition the following yields:

$$J = \frac{\left(1 - v^2\right)}{E}\left(K_I^2 + K_{II}^2\right) + \frac{1}{2G} K_{III}^2 \tag{2.16}$$

The J-Integral corresponds to G and within the framework of LEFM the following expression is valid:

$$G = -\frac{dE}{da} = J, \tag{2.17}$$

where: E = potential energy, J and G, respectively, can be determined by tests under constant load (Fig. 2.7) or fixed displacement (Fig. 2.8).
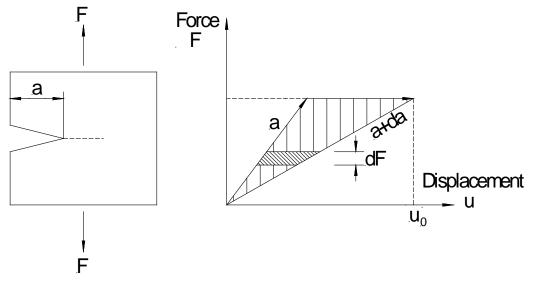

Fig. 2.7: J-Integral determination under constant load (analog to creep test)
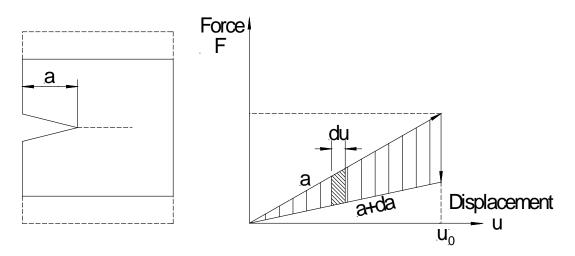

Fig. 2.8: J-Integral determination under fixed displacement (analog to relaxation test)

Introduction into fracture and damage mechanics for rock mechanical applications

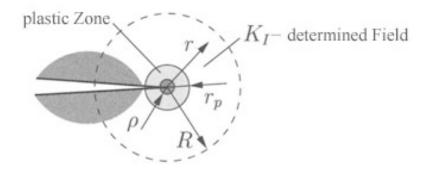Only for private and internal use!   Updated: 4 January 2021

Fig. 2.9: Process (plastic) zone close to crack tip

The shaded area (see Fig. 2.7 and 2.8) corresponds to the change in potential energy, i.e:

$$-\mathrm{d}E = J \cdot \mathrm{d}a \tag{2.18}$$

For the test under constant load the following is valid:

$$J = -\frac{\mathrm{d}E}{\mathrm{d}a} = -\int_0^{F_0}\left(\frac{\partial u}{\partial a}\right)\mathrm{d}F \tag{2.19}$$

For the test under fixed displacement the following holds:

$$J = -\frac{\mathrm{d}E}{\mathrm{d}a} = -\int_0^{u_0}\left(\frac{\partial F}{\partial a}\right)\mathrm{d}u \tag{2.20}$$

The concept of LEFM is valid as long as the process zone (plastified zone at the crack tip) is small compared to the K determined field (e.g. Kuna 2008). If K, G or J reach critical values, critical (fast) fracture propagation starts. K_{Ic}, K_{IIc} and K_{IIIc} are also called fracture toughness. These parameters are material constants and can be determined by special rock mechanical lab tests (e.g. ISRM 2014). Another important parameter in the framework of fracture mechanics is COD (Crack Opening Displacement Δ). Analog to the critical values of K, G and J it is possible for COD to define a critical value. Exemplary, the well-known "Irwin"-model in plane strain should be considered:

$$\Delta = \frac{4\left(1-v^2\right)}{3\pi E}\frac{K_I^2}{\sigma} \tag{2.21}$$

If we furthermore consider, that:

$$G_I = \frac{\left(1-v^2\right)K_I^2}{E}, \tag{2.22}$$

we get from Eq. 2.21 and 2.22:

$$\Delta = \frac{4}{3\pi}\cdot\frac{G_I}{\sigma} \qquad \text{respectively} \qquad G_I = \Delta\cdot\sigma\cdot\frac{3\pi}{4} \tag{2.23}$$

Introduction into fracture and damage mechanics for rock mechanical applications

Only for private and internal use!   Updated: 4 January 2021

These equations demonstrate the equivalence of the parameters *G*, *K* and *COD*. For rocks the following value ranges are valid:

$$K_{Ic} \approx 0.5\ldots3 \text{ MPa}\sqrt{m}$$

$$K_{IIc} \approx 2\ldots15 \text{ MPa}\sqrt{m}$$

$$K_{IIc} > K_{Ic}$$

$$K_{IIc}/K_{Ic} \approx 2\ldots3$$

3   Subcritical crack growth and lifetime

In respect to crack growth processes several phases can be distinguished (Fig. 3.1):
- in respect to fracture propagation velocity: quasi static vs. dynamic
- in respect to fracture toughness: stable vs. unstable

Subcritical crack growth is characterised by very low crack propagation velocity *v*, which follows the relation:

$$v \sim K^n \tag{3.1}$$

$$n \approx 2 \ldots 50 \quad \text{-stress-corrosion-index}$$

The subcritical crack growth can well be described by the so-called „Charles"-equation:

$$v = v_0 \cdot e^{(-H/RT)} \cdot K^n \tag{3.2}$$

where:
v₀   material constant
T   absolute temperature
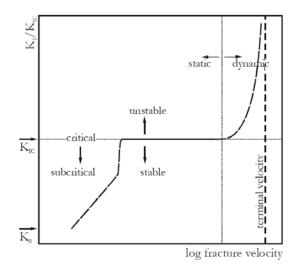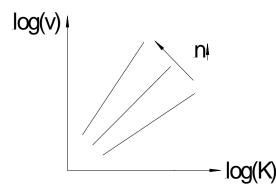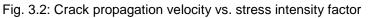*R*   Boltzmann gas constant
H   activation energy

Fig. 3.1: Critical vs. subcritical crack growth

Introduction into fracture and damage mechanics for rock mechanical applications

Only for private and internal use!   Updated: 4 January 2021

Fig. 3.2: Crack propagation velocity vs. stress intensity factor

The logarithm of the „Charles"-equation leads to the following expression:

$$\log v = n \cdot \log K + \log\left(v_0 e^{-(H/RT)}\right)$$
(3.3)

Eq. 3.3 delivers a line in a double-logarithmic diagram, where the stress-corrosion-index n represents the inclination (Fig. 3.2).

The concept of subcritical crack growth can be used to predict lifetime and to simulate/explain the development of damage pattern for rock structures under load, as outlined by Konietzky et al. (2009) and further developed by Li & Konietzky (2014a, b) and Chen & Konietzky (2014). The basic idea within this concept is the existence, growth and coalescence of micro cracks, which leads to the development of macroscopic fractures and finally failure.

4   Apparent fracture toughness

According to the classical fracture mechanical concept (LEFM, see Fig. 2.3) stress at crack tips approaches infinity. On the other hand, according to Eq. 2.10 material strength would approach infinity if it contains no or only infinite small cracks. In practical engineering we should consider different defect types like illustrated in Fig. 4.1.
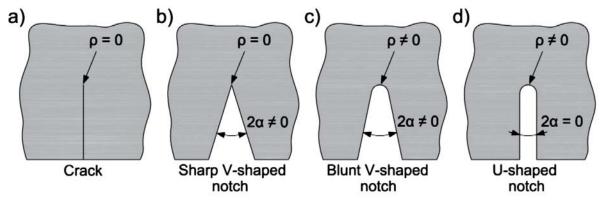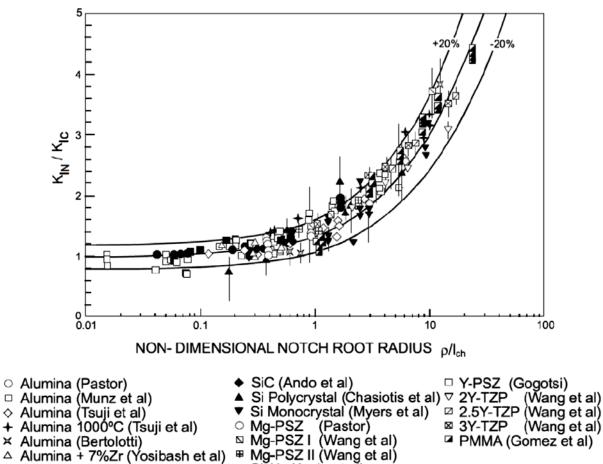

Fig. 4.1: Classification of defect types (Urrutia, 2020)

In a strict sense the classical fracture mechanical concept considers only the situations illustrated in Fig. 4.1a,b. However, in practice notch-type defects with finite radius may

Introduction into fracture and damage mechanics for rock mechanical applications

Only for private and internal use!   Updated: 4 January 2021

dominate and the corresponding apparent fracture toughness K_{IN} is – depend on notch radius – significantly higher (see Fig. 4.2).

Fig. 4.2: Ratio of apparent to classical fracture toughness for different materials and scaled notch radius (Berto & Lazzarin, 2014)

In contrast to Fig. 2.3, the stress in front of the notch shows a behavior like shown in Fig. 4.3. The stress concentration at a notch tip can be separated into 3 zones (Fig. 4.3):

(I)   Zone with nearly constant stress very close to the notch tip (plastified or damaged zone)
(II)   Transition zone
(III)   Linear relation between log(stress) vs. log(distance) like given by Eq. 4.1

$$\sigma_{yy} = \frac{K_\rho}{\left(2 \cdot \pi \cdot r\right)^\alpha} \tag{4.1}$$

where: K_ρ = Notch stress intensity factor (NSIF) , r = distance in front of the notch, α = material constant for given notch radius (α is in the order of 0.5). Please note, that K_ρ varies with notch radius ρ.

Introduction into fracture and damage mechanics for rock mechanical applications

Only for private and internal use!   Updated: 4 January 2021
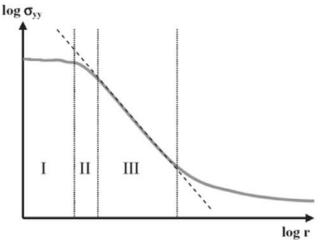

Fig. 4.3: Stress distribution at a notch tip (r = distance from notch tip, σ_{yy} = stress normal to notch length axis; Justo, 2020)
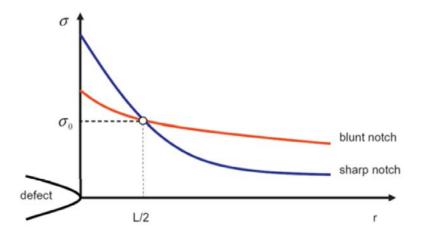
One can define a so-called 'critical distance' L according to the following formula (se also Fig. 4.3):
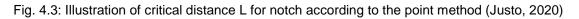
$$L = \frac{1}{\pi}\left(\frac{K_{IC}}{\sigma_0}\right)^2 \qquad (4.2)$$

where σ_0 is the global material strength. L can be considered as an internal material length parameter. There are different methods to determine L. The most popular are:

- point method (PM)
- line method (LM)
- areal method (AM)

The theory of critical distances (TCD) is based on the assumption, that the inherent strength σ_0 is equal to the maximum principal stress calculated either at a certain distance from the notch tip (PM), averaged over a certain distance (LM) or averaged over a certain volume (AM). All of these methods give similar values for L.

Fig. 4.3: Illustration of critical distance L for notch according to the point method (Justo, 2020)

Introduction into fracture and damage mechanics for rock mechanical applications

Only for private and internal use!   Updated: 4 January 2021

The apparent fracture toughness based on L determined according to the PM is written as:

$$K_{IN} = K_{IC} \frac{\left(1 + \dfrac{\rho}{L}\right)^{3/2}}{1 + \dfrac{2\rho}{L}} \tag{4.3}$$

The apparent fracture toughness based on L determined according to the LM is written as:

$$K_{IN} = K_{IC} \sqrt{\frac{\rho}{4L} + 1} \tag{4.4}$$

For $\rho = 0$, both expressions (4.3 and 4.4) describe the sharp crack ($K_{IC} = K_{IN}$).

Fig. 4.4 illustrates the failure envelopes based on LEFM and TCD in comparison with the inherent strength. It documents, that via TCD the defect size dependence of strength can be well described.
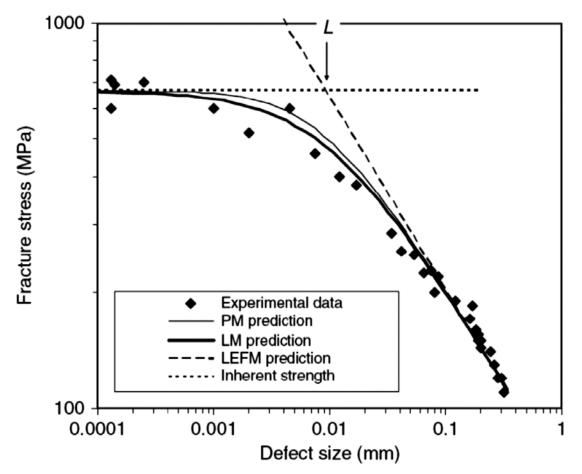

Fig. 4.4: Typical experimental results and predictions according to LEFM and TCD (Taylor, 2004)

Introduction into fracture and damage mechanics for rock mechanical applications

Only for private and internal use!   Updated: 4 January 2021

Fig. 4.5 shows the model set-up for simulating 4-point-bending tests with variable notch radius. The simulations were performed with continuum and discontinuum codes. Like shown in Fig. 4.6, the horizontal stresses along the vertical symmetry line across the notch show a nearly linear trend for larger notch radius (see $\rho = 15$ mm in Fig. 4.6) compared to smaller notch radius (see $\rho = 3$ mm in Fig. 4.6). This indicates that larger notch radius are similar to a simple cross section reduction, whereas smaller notch radii lead to a non-linear increase in stress close to the notch tip.
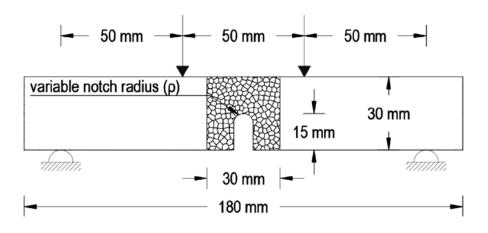

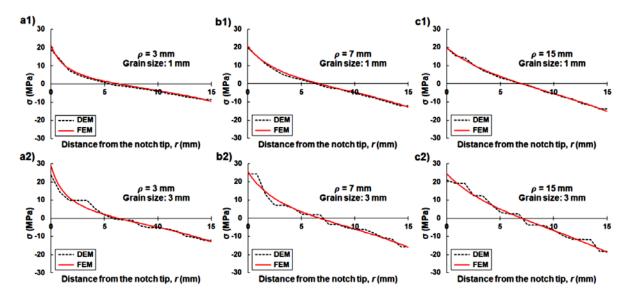Fig. 4.5: Set-up of numerical models for simulation of 4-point-bending tests (Justo & Konietzky, 2020)

Fig. 4.6: Horizontal stresses along the vertical symmetry line across a notch according to Fig. 4.5 (Justo & Konietzky, 2020)

Justo et al. (2020) have also investigated the influence of the grain size via lab testing and numerical simulations using the discrete element method (see Fig. 4.7 and Fig 4.5). Fig. 4.8 confirms again the influence of the notch radius on the apparent fracture toughness, but indicates also the influence of the grain size. Fig. 4.9 documents the dependence of critical distance CT on the grain size which corresponds to Voronoi edge length.

Introduction into fracture and damage mechanics for rock mechanical applications

Only for private and internal use!   Updated: 4 January 2021
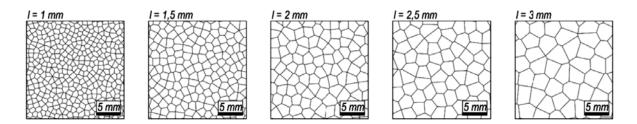
Fig. 4.7: Simulation of varying grain size using Voronoi structure, see also Fig. 4.5 (Justo et al., 2020)
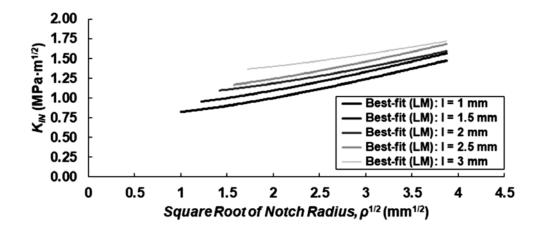

Fig. 4.8: Apparent fracture toughness vs. notch radius for models with different grain size, see also Fig. 4.5 and Fig. 4.7 (Justo et al., 2020)
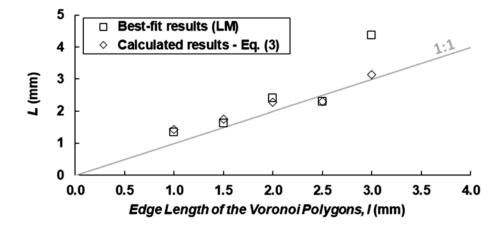

Fig. 4.9: Critical distance versus Voronoi edge length representing the grain size, see also Fig. 4.5 and Fig. 4.7 (Justo et al., 2020)

Introduction into fracture and damage mechanics for rock mechanical applications

Only for private and internal use!   Updated: 4 January 2021

5   Fatigue due to cyclic loading

Except static loading also cyclic loading (load reversal) is an important issue in geo-technical engineering, e.g. for bridge crossing, industrial or traffic vibrations, seismic loading, explosions or blasting. The experience shows that objects exposed to the same load level have longer life time under static loading compared to cyclic loading. Also, it becomes apparent, that rocks under static load level may be stable, while at the same cyclic load level failure is observed. The following different factors have influence on the cyclic fatigue behavior of rocks (Cerfontaine & Collin, 2018):

- frequency
- maximum stress
- stress amplitude
- confinement
- degree of saturation
- anisotropy
- waveform
- sample size

Typical lab tests to investigate the cyclic fatigue behavior of rocks are:

- cyclic uniaxial and triaxial compressive tests
- cyclic indirect (Brazilian) tensile tests
- cyclic 3- and 4-point bending tests

The degree of fatigue is typically characterized by the following damage variables (Song et al., 2018; Cerfontaine & Collin, 2018):

- residual deformation (axial or volumetric)
- wave velocity
- deformation modulus
- AE count or energy
- dissipated energy / energy ratio
- permeability

The most classical and still often used representation of the cyclic fatigue behavior is the so-called S-N (Wöhler) curve, which results in a straight line if a semi-logarithmic plot is used. The S-N curve relates the number of cycles N up to failure to the normalized ratio of maximum cyclic stress σ_{max} to monotonic strength σ_{mon} (A and B are material parameters):

$$\frac{\sigma_{max}}{\sigma_{min}} = A \cdot \log_{10} N - B \tag{5.1}$$

For sinusoidal excitation the parameters shown in Fig. 5.1 are given, where N is defined as the number of cycles and K as the stress intensity factor. According to Fig. 5.1 the following definitions are valid:

$$\Delta K = K_{max} - K_{min}$$

$$K_m = \frac{K_{max} + K_{min}}{2}$$

$$R = \frac{K_{min}}{K_{max}}$$

(5.2)

The increment in fracture length per loading cycle (da/dN) can be represented in a logarithmic plot (Fig. 5.2), where ΔK_{th} represents the stress intensity factor magnitude, below which no crack propagation occurs and ΔK_c represents the critical stress intensity factor magnitude, where critical crack propagation starts.
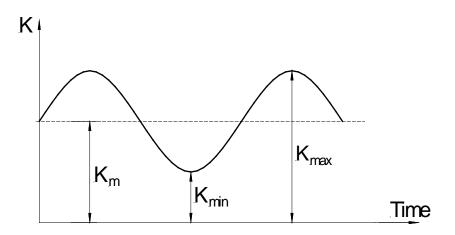

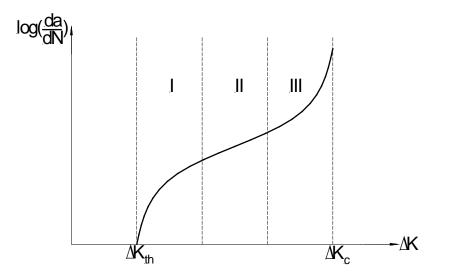Fig. 5.1: Basic fracture mechanical parameters for cyclic loading

Fig. 5.2: Phases of crack propagation under cycylic loading

Crack propagation within phase I can be described by the „Donahne" law:

$$\frac{da}{dN} = K\left(\Delta K - \Delta K_{th}\right)^{m}$$

(5.3)

where: $\Delta K_{th} = \left(1 - R\right)^{\gamma} \Delta K_{th,\,0}$

(5.4)

Introduction into fracture and damage mechanics for rock mechanical applications

Only for private and internal use!   Updated: 4 January 2021

$\Delta K_{th\,0}$ is the threshold for $R = 0$ and γ is a material parameter.

Crack propagation within phase II is given by the „Paris-Erdogan"-relation:

$$\frac{\mathrm{d}a}{\mathrm{d}N} = C(\Delta K)^m \tag{5.5}$$

m and C are material constants, where m is often set to 4.

Crack propagation within phase III can be described by the "Forman" law:

$$\frac{\mathrm{d}a}{\mathrm{d}N} = \frac{C \cdot (\Delta K)^n}{(1 - R)\,K_c - \Delta K} \tag{5.6}$$

C and n are material constants.

An expression, which covers all three phases is the so-called „Erdogan and Ratwani" law:

$$\frac{\mathrm{d}a}{\mathrm{d}N} = \frac{C(1 + \beta)^m \cdot (\Delta K - \Delta K_{th})^n}{K_c - (1 + \beta)\,\Delta K} \tag{5.7}$$

where $\beta = \dfrac{K_{max} + K_{min}}{K_{max} - K_{min}}$ and c, m, n are material constants. $\tag{5.8}$

6   Introduction into Continuum Damage Mechanics (CDM)

Instead of considering the stress-strain or force-displacement relation of crack or fractures in detail, CDM considers the overall damage in terms of smeared parameters and can handle infinite number of defects. Within the CDM concept, damage is expressed by any kind of defects, like pores, cracks, planes of weakness etc. and is given by the damage variable D, which can be defined in different ways depending on the applied approach and problem. Eq. 6.1 gives a volumetric definition, whereas Eq. 6.2 gives an area definition for a fictitious cross section through the body.

$$D = \frac{V_{Pore}}{V_{Total}} \qquad V = \text{Volume} \tag{6.1}$$

$$D = \frac{A_{Pore}}{A_{Total}} = \frac{A_P}{A_T} \qquad A = \text{Cross sectional area} \tag{6.2}$$

For the damage variable holds $0 \leq D \leq 1$, i.e. $D = 0$ indicates no damage at all and $D = 1$ means 100 % damaged. The damage variable D can be a scalar (isotropic damage) or a tensor (anisotropic damage):

Isotropic damage: $D = \dfrac{A_P}{A_G}$ $\tag{6.3}$

Anisotropic damage: $\left(\delta_{ij} - D_{ij}\right) n_j\, dA = \tilde{n} \cdot d\bar{A}$ (6.4)

By means of the damage variable D effective stresses can be determined. For isotropic damage under uniaxial load the following can be deduced (A_G = total area, A_P = pore area):

$$\sigma^{eff} = \frac{\sigma}{1-D} \qquad \text{because} \qquad \sigma = \frac{F}{A} = \frac{F}{A_G - A_P} \qquad (6.5)$$
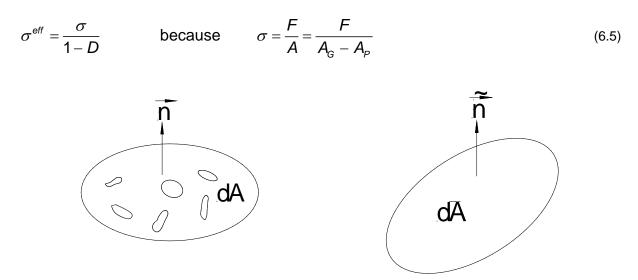

Fig. 6.1: Illustration for definition of anisotropic damage (left: reference configuration, right: equivalent (deformation-equivalent) continuum configuration.The operator ($\delta_{ij} - D_{ij}$) transforms the reference configuration into an equivalent continuum mechanical configuration without defects, but with smaller area and modified normal vektor n.

$$= \frac{\dfrac{F}{A_G}}{1 - \dfrac{A_P}{A_G}} = \frac{\sigma}{1-D} \qquad (6.6)$$

Isotropic damage under polyaxial load is defined by:

$$\sigma_{ij}^{eff} = \frac{\sigma_{ij}}{1-D} \qquad (6.7)$$

Damage can also be interpreted by reduced stiffness, e.g. reduced Young's modulus. If one assumes identical macroscopic stresses and identical macroscopic deformation, the following equations can be deduced ($\bar{E}$ = Young's modulus of damaged material, E = Young's modulus of undamaged material):

$$\varepsilon = \frac{\sigma}{\bar{\bar{E}}} = \frac{\sigma}{E} = \frac{F}{A_G \cdot \bar{\bar{E}}} = \frac{F}{\left(A_G - A_P\right) \cdot E} \qquad (6.8)$$

Introduction into fracture and damage mechanics for rock mechanical applications

Only for private and internal use! Updated: 4 January 2021

This implies that:

$$A_G \cdot \bar{E} = \left(A_G - A_p \right) \cdot E$$

$$\bar{E} = \frac{A_G - A_p}{A_G} \cdot E \tag{6.9}$$

$$\bar{E} = (1 - D) \cdot E \qquad \text{or} \qquad D = 1 - \frac{\bar{E}}{E}$$

As a consequence the elastic law for damaged material can be deduced:

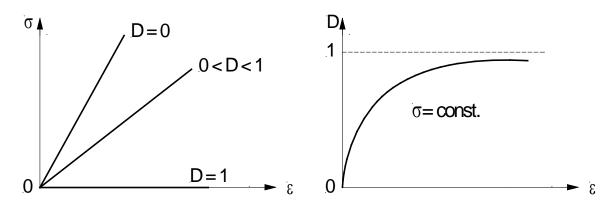$$\sigma = E (1 - D) \cdot \varepsilon \tag{6.10}$$

Fig. 6.2: Illustration of stress-strain relation of damaged and undamaged material (left) and damage development versus deformation under constant load (right).

Damage can be detected by measuring changes in ultrasonic wave speed, for instance by measuring longitudinal wave speed:

$$D = 1 - \frac{\bar{E}}{E} = 1 - \left[\frac{\dfrac{\bar{V}_P^2 \cdot \bar{\rho} \left(1 + v \right) \left(1 - 2v \right)}{1 - v}}{\dfrac{V_P^2 \cdot \rho \left(1 + v \right) \left(1 - 2v \right)}{1 - v}} \right] = 1 - \frac{\bar{V}_P^2 \cdot \bar{\rho}}{V_P^2 \cdot \rho} \tag{6.11}$$

Because changes in density ρ as a general rule a negligible small, Eq. 6.11 can be simplified as follows:

$$D \approx 1 - \frac{\bar{V}_P^2}{V_P^2} \tag{6.12}$$

Corresponding graphical presentations of the damage process in general are shown in Fig. 6.2 for a rock specimen under compressive load.

Introduction into fracture and damage mechanics for rock mechanical applications

Only for private and internal use!   Updated: 4 January 2021

Three thresholds have to be considered:

    1.) no damage:

$$\text{for } \varepsilon < \varepsilon^*: \quad D = 0, \quad \begin{aligned} E &= \overline{\overline{E}} \\ \sigma &= \overline{\sigma} \end{aligned} \tag{6.13}$$

    2.) Start of microcrack growth, i. e. onset of damage

$$\text{for } \varepsilon > \varepsilon^*: \quad D \text{ increasing}, \quad \begin{aligned} E &\neq \overline{\overline{E}} \\ \sigma &\neq \overline{\sigma} \end{aligned} \tag{6.14}$$

    3.) Start of macroscopic crack growth, i. e. macroscopic fracture mechanics

$$\text{for } \varepsilon > \varepsilon^{**}: \quad D = D_c \tag{6.15}$$

Damage in terms of microscopic crack growth takes place for:

$$\varepsilon^* < \varepsilon < \varepsilon^{**} \quad \text{or} \quad \sigma^* < \sigma < \sigma^{**} \tag{6.16}$$

Damage in terms of CDM leads to the following practical consequences:
- Reduction of Young's modulus
- Reduction of elastic wave velocities
- Reduction of density
- Increase of creep rate

Introduction into fracture and damage mechanics for rock mechanical applications

Only for private and internal use!   Updated: 4 January 2021

7   Stochastic view (Weibull-Model)

The probability of failure according to the "Weibull" concept (e.g. Liebowitz 1968) is based on the following assumptions:

- statistical homogenous distribution of defects
- „weakest link theory", i. e. failure of the whole considered structure, if the weakest single defect fails
- no interaction between defects

The probability of failure is given by:

$$p_f = F(\sigma) = 1 - \exp\left[-\frac{V}{V_0}\left(\frac{\sigma^*}{\sigma_0}\right)^m\right] \tag{7.1}$$

where:

V_0 = elementary volume

V = considered volume

σ_0 = average strength (stress value at which 63,2 % of all samples fail)

m = Weibull parameter ($\sim 1 - 40$) is a measure for the variance of the strength parameter (the bigger m, the closer the strength values lie together)

σ^* = effective stress

with $\sigma^* = \sigma(1-D)$ the following expression can be deduced:

$$P_f = 1 - \exp\left[-\frac{V}{V_0}\left(\frac{\sigma(1-D)}{\sigma_0}\right)^m\right] \tag{7.2}$$

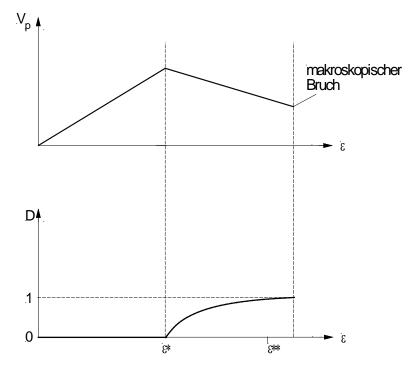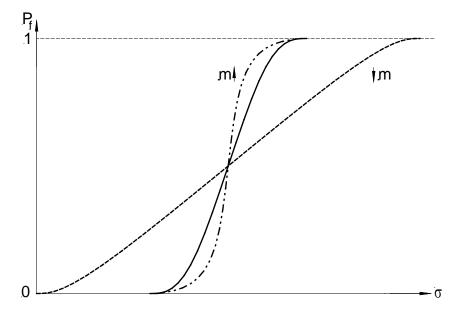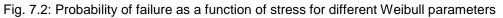Fig. 7.1: Principal history for damage and wave speed with ongoing deformation for a rock specimen with softening under compressive load

Introduction into fracture and damage mechanics for rock mechanical applications

Only for private and internal use! Updated: 4 January 2021

Fig. 7.2: Probability of failure as a function of stress for different Weibull parameters

The Weibull distribution can be used to manifest the scale effect, as outlined below. The 2-parametric Weibull distribution can be used to describe the distribution of defects (pores, cracks, flaws, notches etc.):

$$F(a) = e^{-\left(\frac{a}{a_c}\right)^b} \tag{7.3}$$

where:

a_c = characteristic defect size (e.g. crack length, pore radius)
b = variance parameter
$F(a)$ = probability, that within the considered volume V_0 a defect $\leq a$ exist.

Within a n-time bigger volume V:

$$V = n \cdot V_0 \tag{7.4}$$

due to the series connection of failure elements the following holds:

$$F_v(a) = \sum_{i=1}^{n} \{F(a)\} = e^{-n\left(\frac{a}{a_c}\right)^b} \tag{7.5}$$

If one inserts Eq. 7.4 into Eq. 7.5 one obtains:

$$F_v(a) = e^{-\frac{V}{V_0} \cdot \left(\frac{a}{a_c}\right)^b} \tag{7.6}$$

Eq. 7.6 can be interpreted in such a way, that the characteristic defect size a_c increases with increasing volume. Under the assumption that local stress concentrations (notch stresses, stresses at crack tips etc.) are crucial for failure, one can write:

Introduction into fracture and damage mechanics for rock mechanical applications

Only for private and internal use! Updated: 4 January 2021

$$\sigma \sim \frac{1}{\sqrt{a}} \tag{7.7}$$

and can insert expression 7.7 into Eq. 7.6:

$$F_G(\sigma) = e^{-\frac{V}{V_0}\left(\frac{\sigma_0}{\sigma}\right)^b} = e^{-\frac{V}{V_0}\left(\frac{\sigma}{\sigma_0}\right)^{b_\sigma}} \tag{7.8}$$

For identical failure probabilities holds:

$$\frac{V}{V_0} \cdot \left(\frac{a}{a_c}\right)^b = \text{const.} = K. \tag{7.9}$$

and after rearrangement:

$$\frac{a}{a_c} = K \cdot \left(\frac{V_0}{V}\right)^{\frac{1}{b}} \tag{7.10}$$

It can be concluded from Eq. 7.10, that the characteristic size of defects increases with increasing volume (V increases $\rightarrow$ a_c increases). Analog to Eq. 7.8 an expression based on stresses can be formulated:

$$\frac{V}{V_0} \cdot \left(\frac{\sigma}{\sigma_0}\right)^{b_\sigma} = \text{const.} = K \tag{7.11}$$

Eq. 7.11 can be interpreted in such a way, that characteristic local stress concentrations increase with increasing volume and therefore a lower stress level will lead to failure.

Introduction into fracture and damage mechanics for rock mechanical applications

Only for private and internal use!   Updated: 4 January 2021

8   Literature

Anderson, T.L. (2004): Fracture Mechanics – Fundamentals and Applications, CRC Press

Atkinson, B.K. (1991): Fracture Mechanics of Rock, Academic Press

Berto, F. & Lazzarin, P. (2014): Recent developments in brittle and quasi-brittle failure assessment of engineering materials by means of local approaches, Theoretical and Applied Fracture Mechanics, 52(3): 183-194

Cerfontaine, B., Collin, F. (2018): Cyclic and fatigue behaviour of rock material: review, interpretation and research perspective, RMRE, 51(2): 391-414

Chen, W. & Konietzky, H. (2014): Simualtion of heteroneity, creep, damage and lifetime for loadad britte rocks, Tectonophysics, http://dx.doi.org/10.1016/j.tecto.2014.06.033

Gdoutos, E.E. (2005): Fracture Mechanics, Springer

Gross, D. & Seelig, Th. (2001): Bruchmechanik, Springer

Hellan, K. (1984): Introduction to Fracture Mechanics, McGraw-Hill

ISRM (2014): ISRM Suggested Methods, http://www.isrm.net/gca/?id=177 (29.06.2015)

Justo, J. (2020): Fracture assessment of notched rocks under different loading and temperature conditions using local criteria, PhD Thesis, University of Cantabria

Justo, J. & Konietzky, H. (2020): Voronoi based discrete element analysis to assess the influence of the grain size on the apparent fracture toughness of notched rock specimens, ARMA 20: 1467

Justo, J., Konietzky, H., Castro, J. (2020): Discrete numerical analyses of grain size influence on the fracture of notched rock beams. Computer and Geotechnics, 125: 103680

Konietzky et al. (2009): Lifetime prediction for rocks under static compressive and tensile loads – a new simulation approach, Acta Geotechnica, 4: 73-78

Kuna, M. (2008): Numerische Beanspruchungsanalyse von Rissen, Vieweg + Teubner

Lemaitre, J & Desmorat, R. (2005): Engineering Damage Mechanics, Springer

Li, X. & Konietzky, H. (2014 a): Time to failure prediction scheme for rocks, Rock Mechanics Rock Engineering, 47: 1493-1503

Li, X. & Konietzky, H. (2014 b): Simulation of time-dependent crack growth in brittle rocks under constant loading conditions, Engineering Fracture Mechanics, 119: 53-65

Liebowitz, H. (1968): Fracture – An Advanced Treatice, Vol II: Mathematical Fundamentals, Academic Press

Song, Z., Konietzky, H., Frühwirt, T. (2018): Hysteresis energy-based failure indicators for concrete and brittle rocks under the condition of fatigue loading, Int. Journal of Fatigue, 114: 298-310

Taylor, D. (2004): Predicting the fracture strength of ceramic material using the theory of critical distances, Engineering Fracture Mechanics, 71: 2407-2416